A HERG-like K^+ channel in rat F-11 DRG cell line: pharmacological identification and biophysical characterization

Laura Faravelli, Annarosa Arcangeli*, Massimo Olivotto* and Enzo Wanke†

*Department of General Physiology and Biochemistry, University of Milano, Via Celoria 26, I-20133 Milano and *Institute of General Pathology, University of Firenze, Viale Morgagni 50, I-50134 Firenze, Italy*

1. The relationships between the K^+ inward rectifier current present in neuroblastoma cells (I_{IR}) and the current encoded by the human *ether-á-go-go*-related gene (*HERG*), I_{HERG}, and the rapidly activating repolarizing cardiac current $I_{K(r)}$, were investigated in a rat dorsal root ganglion (DRG) × mouse neuroblastoma hybrid cell line (F-11) using pharmacological and biophysical treatments.

2. I_{IR} shared the pharmacological features described for $I_{K(r)}$, including the sensitivity to the antiarrhythmic drugs E4031 and WAY-123,398, whilst responding to Cs^+, Ba^{2+} and La^{3+} in a similar way to I_{HERG}.

3. The voltage-dependent gating properties of I_{IR} were similar to those of $I_{K(r)}$ and I_{HERG}, although I_{IR} outward currents were negligible in comparison.

4. In high K^+ extracellular solutions devoid of divalent cations, I_{IR} deactivation kinetics were removed resulting in long-lasting currents apparently activated in hyperpolarization, with a marked (2·7-fold) increase in conductance, as recorded from the instantaneous linear current–voltage relationship at −120 mV. Re-addition of Ca^{2+} restored the original closure of the channel whereas re-addition of Mg^{2+} reduced the peak current.

5. The I_{IR} described here, the heart $I_{K(r)}$ and the I_{HERG} could be successfully predicted by a unique kinetic model where the voltage dependencies of the activation/inactivation gates were properly voltage shifted. On the whole, I_{IR} seems to be the first example of a HERG-type current constitutively expressed and operating in mammalian cells of the neuronal lineage.

The human *ether-á-go-go*-related gene (*HERG*), identified from a hippocampal cDNA (Warmke & Ganetzky, 1994), encodes a peptide which, upon expression in *Xenopus* oocytes, produces a K^+ current (I_{HERG}; Sanguinetti, Jiang, Curran & Keating, 1995; Trudeau, Warmke, Ganetzky & Robertson, 1995; Smith, Baukrowitz & Yellen, 1996; Schönherr & Heinemann, 1996), which has quite similar biophysical features to, but not all the pharmacological properties of, $I_{K(r)}$, a K^+ current which initiates repolarization of heart action potentials (Shibasaki, 1987; Sanguinetti & Jurkiewicz, 1990*a*). Consistently, *HERG* mutations cause one inherited cardiac arrhythmia, characterized by QT prolongation on electrocardiogram, the long-QT syndrome (LQT2) (Curran, Splawski, Timothy, Vincent, Green & Keating, 1995). Class III antiarrhythmic agents, such as sotalol, a benzenesulphonamide β-blocker, and its analogue E4031 (1-[2-(6-methyl-2-pyrydinil)ethyl]-4-(4-methylsulphonylaminobenzoyl) piperidine), strongly contribute to the isolation of $I_{K(r)}$, which is selectively blocked by these agents. $I_{K(r)}$ was interpreted as a delayed rectifier K^+ current endowed with an extremely fast inactivation, responsible for the rectification (Sanguinetti & Jurkiewicz, 1990*a*).

A very similar current (I_{IR}), with a sensitivity to Cs^+ and Ba^{2+} identical to that described for I_{HERG} by Trudeau *et al.* (1995), was recently discovered in neuroblastoma cells (Arcangeli *et al.* 1993, 1995). I_{IR} turned out to be a K^+ inward-rectifier current, involved in adhesion-mediated neuritogenesis and modulated by the cell cycle.

This current was interpreted by introducing a hyperpolarization-activated opening gate ($m(V)$) and a depolarization-activated inactivation gate ($h(V)$), in a model which is in fact specular to that used so far to interpret $I_{K(r)}$ and I_{HERG} (Sanguinetti & Jurkiewicz, 1990*a*). The possibility of specular interpretations of channel voltage

† To whom correspondence should be addressed.

gating has been recently shown by the demonstration that it is possible to change some outward rectifier channels into inward rectifiers with triple mutations (Miller & Aldrich, 1996). In this case, the inactivation gate of the outward rectifier may be regarded as the activation gate of the inward rectifying channel. This equivalence was adopted by us in Arcangeli *et al.* (1995) with the implicit convention that inactivation of the inward rectifier channel is deactivation of the outward rectifier.

However, recent site-directed mutagenesis experiments (Smith *et al.* 1996; Schönherr & Heinemann, 1996) provided evidence that the very fast inactivation mechanism invoked to explain the apparent inward rectification of HERG can be removed, a fact that makes it difficult to apply to HERG-like currents the specular model we used to describe I_{IR}.

We show here that in the rat dorsal root ganglion (DRG) × mouse neuroblastoma hybrid F-11 clone (Platika, Boulos, Baizer & Fishman, 1985; Boland & Dingledine, 1990), I_{IR} was blocked by specific inhibitors of $I_{K(r)}$ such as E4031 (Sanguinetti *et al.* 1990*a*) and by WAY-123,398 (WAY, [(4-methylsulphonyl)amido]benzenesulphonamide), another class III antiarrhythmic agent (Spinelli, Moubarak, Parsons & Colatsky, 1993). Moreover, unlike $I_{K(r)}$ in heart and I_{HERG} in oocytes, our tumour cell current displayed a weak outward amplitude as compared with the inward. Although some of the novel behaviour of I_{IR} in F-11 cells bathed in solutions devoid of divalent cations are difficult to reconcile with the classical interpretation of $I_{K(r)}$, we developed a comprehensive model which describes I_{IR} according to the convention adopted by Sanguinetti *et al.* (1990*a*).

METHODS

Cell culture

Cells of the F-11 clone (mouse neuroblastoma N18TG-2 × rat DRG; Platika *et al.* 1985; Boland & Dingledine, 1990) were routinely cultured in Dulbecco's modified Eagle's medium (DMEM), containing 4·5 g l^{-1} glucose and 10% fetal calf serum (FCS). The cells were incubated at 37 °C in a humidified atmosphere with 10% CO_2.

Solutions

Extracellular solutions were delivered by hypodermic needles inserted into a capillary tube with a small hole (0·4 mm) positioned near the cell under study. The standard extracellular solution contained (mM): NaCl, 130; KCl, 2; $CaCl_2$, 2; $MgCl_2$, 2; Hepes–NaOH, 10; glucose, 5; pH 7·4. When required, NaCl was replaced with KCl. The solutions used in Figs 5 and 6 contained 120 mM KCl with 5 mM EGTA, or 120 mM KCl with 2 mM of either $CaCl_2$ or $MgCl_2$ and were prepared with extremely pure KCl salts (Aristar grade, BDH, UK; Ca^{2+}, 0·1 p.p.m.; Mg^{2+}, 0·05 p.p.m.) in order to reduce possible contamination with Ca^{2+} or Mg^{2+} in the absence of EGTA. The standard pipette solution at a $[Ca^{2+}]_i$ of 10^{-7} M (pCa 7) contained (mM): potassium aspartate, 120; NaCl, 10; $MgCl_2$, 2; $CaCl_2$, 4; EGTA–KOH, 10; Hepes–KOH, 10; MgATP, 3; Na_2GTP, 0·2.

Antiarrhythmic drugs

E4031 (Sanguinetti *et al.* 1990*a*) and WAY-123,398 (WAY, Spinelli *et al.* 1993) were dissolved in distilled water to make 10 mM stock solutions. E4031 was a generous gift from Dr D. Nisato, Sanofi Recherche, Montpellier, France. WAY was received from Dr W. Spinelli, Wyeth-Ayerst Research, Princeton, NJ, USA.

Patch-clamp recordings

Currents were recorded at room temperature as described (Arcangeli *et al.* 1993, 1995). We carefully compensated pipette resistance (4–6 MΩ), cell capacitance and the series resistance errors by introducing a compensation of about 85–95% before each voltage clamp protocol run. When necessary, membrane potential was measured in current-clamp mode ($I = 0$). During acquisition and data analysis, the pCLAMP (Axon Instruments) and Origin 4.0 (Microcal Inc., Northampton, MA, USA) software was routinely used on 486DX2 PCs (Vobis, Monza, Italy).

Analysis and I_{IR} model prediction

The predictions performed in Fig. 7 followed the classical scheme (Shibasaki, 1987; Sanguinetti & Jurkiewicz, 1990*a*) used to interpret $I_{K(r)}$. Such a scheme describes currents as the product of the two voltage-dependent variables $n(V)$ and $R(V)$ according to the following equation:

$$I_{IR} \text{ or } I_{HERG} = g_{max} \times n(V) \times R(V) \times (V_m - E_K), \quad (1)$$

where g_{max} represents maximal chord conductance, V_m, membrane potential and E_K, potassium reversal potential. We used the classical formalism of Hodgkin & Huxley (1952) with the following forward (α) and backward (β) rate constants:

For the IR submodel (Fig. 7, bottom 2 rows) the rates were:

$$\alpha_R = 30/\{1 + \exp[0{\cdot}04(V + 245)]\},$$
$$\alpha_n = 0{\cdot}09/\{1 + \exp[0{\cdot}011(V + 120)]\},$$
$$\beta_R = 0{\cdot}15/\{1 + \exp[-0{\cdot}05(V + 120)]\},$$
$$\beta_n = 0{\cdot}00035\exp[0{\cdot}07(V + 25)].$$

For the HERG submodel (Fig. 7, top 2 rows) the following rates were used:

$$\alpha_R = 30/\{1 + \exp[0{\cdot}04(V + 215)]\},$$
$$\alpha_n = 0{\cdot}022/\{1 + \exp[0{\cdot}11(V + 100)]\},$$
$$\beta_R = 0{\cdot}15/\{1 + \exp[-0{\cdot}05(V + 120)]\},$$
$$\beta_n = 0{\cdot}00035\exp[0{\cdot}07(V + 25)].$$

All the reconstructions of Fig. 7 were obtained with the program Axon Engineer Pro from AEON Software, Madison, WI, USA.

RESULTS

The voltage-dependent properties of I_{IR} activation and inactivation in F-11 cells

The exemplary properties of I_{IR} activation are illustrated in Fig. 1*A* for an F-11 cell. Inward currents were elicited from a holding potential of 0 mV. The inactivation curve $R(V)$ was obtained by plotting the normalized peak chord conductance ($g_{peak} = I_{IR,peak}/(V_m - E_K)$) *versus* the membrane potential V_m (□). To study the activation gate, we used the protocol reported in Fig. 1*B*, starting from a holding potential of 0 mV, and testing I_{IR} at −120 mV, after preconditioning from −10 to −60 mV for 16 s. The tail currents elicited at −120 mV (shown in Fig. 1*C*) were normalized to obtain the activation curve $n(V)$ illustrated in Fig. 1*D*.

On the whole, these data do not essentially differ from those described for other neuroblastoma clones (Arcangeli *et al.* 1995), provided that the change in the nomenclature of the voltage-dependent gates is taken into account ($R(V) = m(V)$ and $n(V) = h(V)$).

The comparison of I_{IR} with reported recordings of $I_{K(r)}$ and I_{HERG}

The recordings of Fig. 1 were indeed very similar to the tail currents attributed to $I_{K(r)}$ (see Shibasaki, 1987, Fig. 1 at 50 mM K_o^+) and I_{HERG} (Sanguinetti *et al.* 1995, Fig. 5, 10 mM K_o^+; Trudeau *et al.* 1995, Figs 1*D* and 4*A* in high K^+ Ringer solution). This prompted us to explore the outward component of I_{IR} in order to strengthen this comparison. We investigated the K^+ conductances of F-11 cells in the physiological range of V_m with a protocol similar to those used to characterize I_{HERG} (Sanguinetti *et al.* 1995; Trudeau *et al.* 1995) (Fig. 2*A*). Inward currents were not observed in this range, while outward currents elicited positive to 0 mV had the same features as the slowly inactivating delayed rectifier currents (I_{DR}) present in neuroblastoma cells (Arcangeli *et al.* 1995). Slowly activating currents, like those registered for I_{HERG}, (Sanguinetti *et al.* 1995) were constantly absent in our recordings. The repolarization to −120 mV elicited large inward currents (see inset) resembling the tail currents described for I_{HERG} (Sanguinetti *et al.* 1995; Trudeau *et al.* 1995). Interestingly, we also obtained (at −120 mV) inward currents behaving as those shown in Fig. 1*C* with this protocol.

In a previous study (Arcangeli *et al.* 1995), we found that in all tested neuroblastoma cell lines I_{IR} was blocked by Cs^+ and Ba^{2+} with a dose and voltage dependence very similar to those reported for I_{HERG} (Trudeau *et al.* 1995). In F-11 cells, the addition of 5 mM Cs^+ completely blocked I_{IR} without effects on outward components (Fig. 2*B*). To explore further the possible presence of outward I_{IR}, we tested the effects of 10 mM tetraethylammonium (TEA), a general blocker of K^+ currents (Fig. 2*C*). The drug almost completely blocked the outward currents and only partially blocked the inward currents elicited at −120 mV. The further addition of Cs^+ (in TEA) let us isolate (by subtraction) a Cs^+-sensitive component (smaller than in control, Fig. 2*A*), which again displayed only an inward component (see inset to Fig. 2*C*).

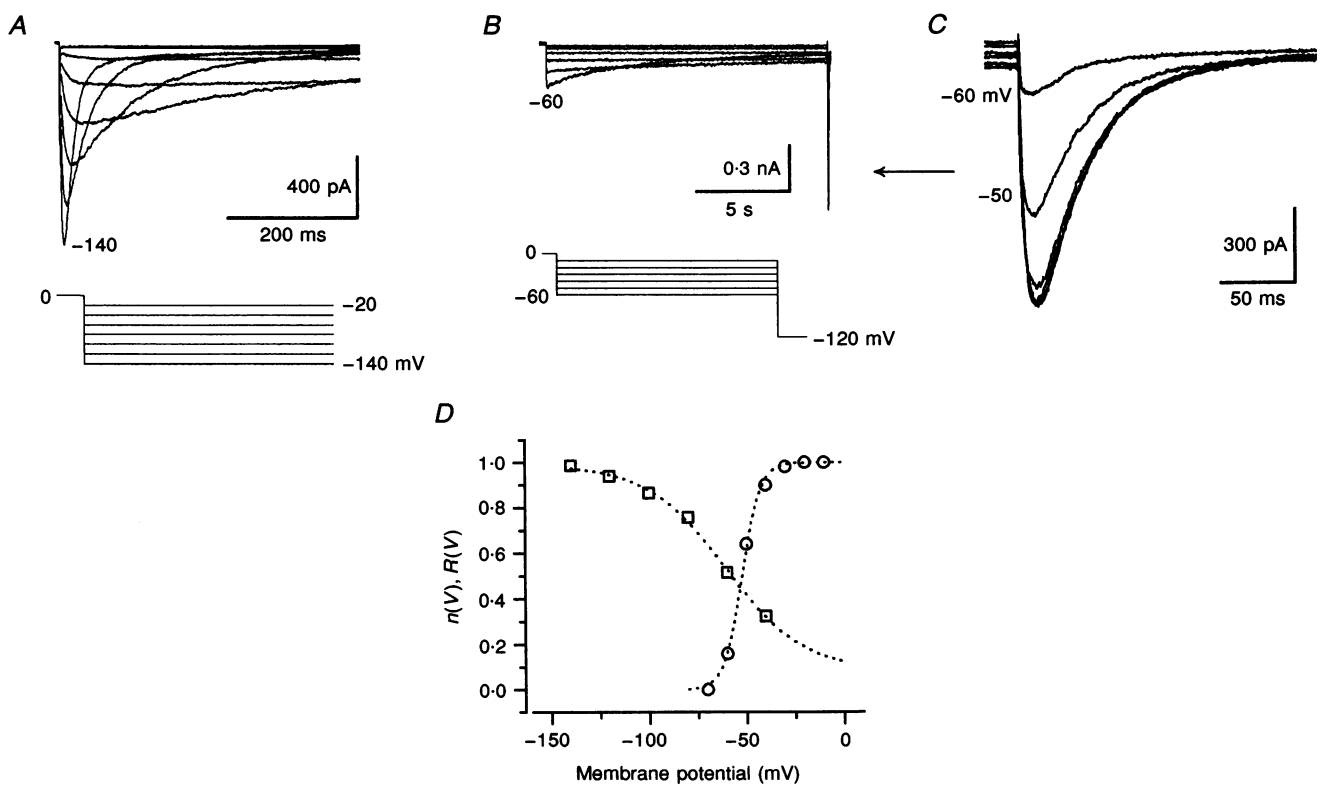

Figure 1. Inwardly rectifying currents, I_{IR}, recorded in F-11 cells

A, currents elicited at various V_m (from −20 to −140 mV) from a holding potential (V_h) of 0 mV. After fitting the decaying currents, the time constants at −140, −120, −100 and −80 mV were: 18, 40, 109 and 412 ms, respectively. *B*, currents obtained during long preconditioning voltage steps (from −10 to −60 mV) from V_h of 0 mV and tested at −120 mV. *C*, the currents elicited at −120 mV in *B*. *D*, voltage-dependent variables $R(V)$ (□) and $n(V)$ (○) obtained from data in *A–C*. $R(V)$ and $n(V)$ were obtained by normalizing the peak chord conductance (g/g_{max}) and the peak current (I/I_{max}) respectively. Dotted lines are Boltzmann curves which best fitted to the data with $V_{½}$ and slope as follows (mV): $n(V)$, −52, 4·8; $R(V)$, −57, 24. $[K^+]_o$ was 40 mM, which sets the Nernst equilibrium potential to about −30 mV.

Although these pharmacological treatments suggested that the outward component of I_{IR} is very small compared with the inward current, we adopted the envelope of tails test (Noble & Tsien, 1969; Sanguinetti *et al.* 1990*a*) to verify that (i) the inward I_{IR} is a single current, and (ii) the large outward currents in F-11 cells are not related to I_{IR}. The envelope of tails test predicts that, if a current is sustained by a single channel, then the magnitude of tail currents after a given depolarizing pulse of variable duration should increase in parallel to the time course of activation of outward current during the pulse. Under these conditions, the ratio of the tail current, $I_{tail}(t)$, to the time-dependent current $I(t)$ should be constant, regardless of the pulse duration. By using the protocol shown in Fig. 2*D* inset, but changing the preconditioning time (0·3 to 10 s), we produced the recordings shown in Fig. 2*D*, obtaining a constant ratio $I_{tail}(t)/I(t)$ (Fig. 2*F*, □). The value (2·85 ± 0·2) is close to the predicted ratio (3), calculated from the ratio of the driving forces at $V_{test} = -120$ and -60 mV for a K^+ selective channel at $[K^+]_o = 40$ mM (theoretical $E_K = -30$ mV). Moreover, the same test adopted for the outward component of $I(t)$ (elicited by the protocol shown in Fig. 2*E*) did not give a constant value (Fig. 2*F*, ○). In contrast, although the ratio starts at the expected value (−1·85) for a single outward current elicited by the adopted protocol (Fig. 2*E*, inset), it falls rapidly to more negative values with the increase of the pulse duration, i.e. with the appearance of the inward component. This result rules out the assumption that the bulk of outward currents registered are components of the same current as I_{IR}.

On the whole these results show that I_{IR} should have a very small component of outward current as compared to that reported for $I_{K(r)}$ and I_{HERG} (Sanguinetti *et al.* 1990*a*, 1995; Trudeau *et al.* 1995, but see Smith *et al.* 1996; Schönherr & Heinemann, 1996, where the outward currents are smaller). Nevertheless, this I_{IR} component is decisive in the setting of the resting potential (V_{rest}) (Arcangeli *et al.* 1993, 1995), so

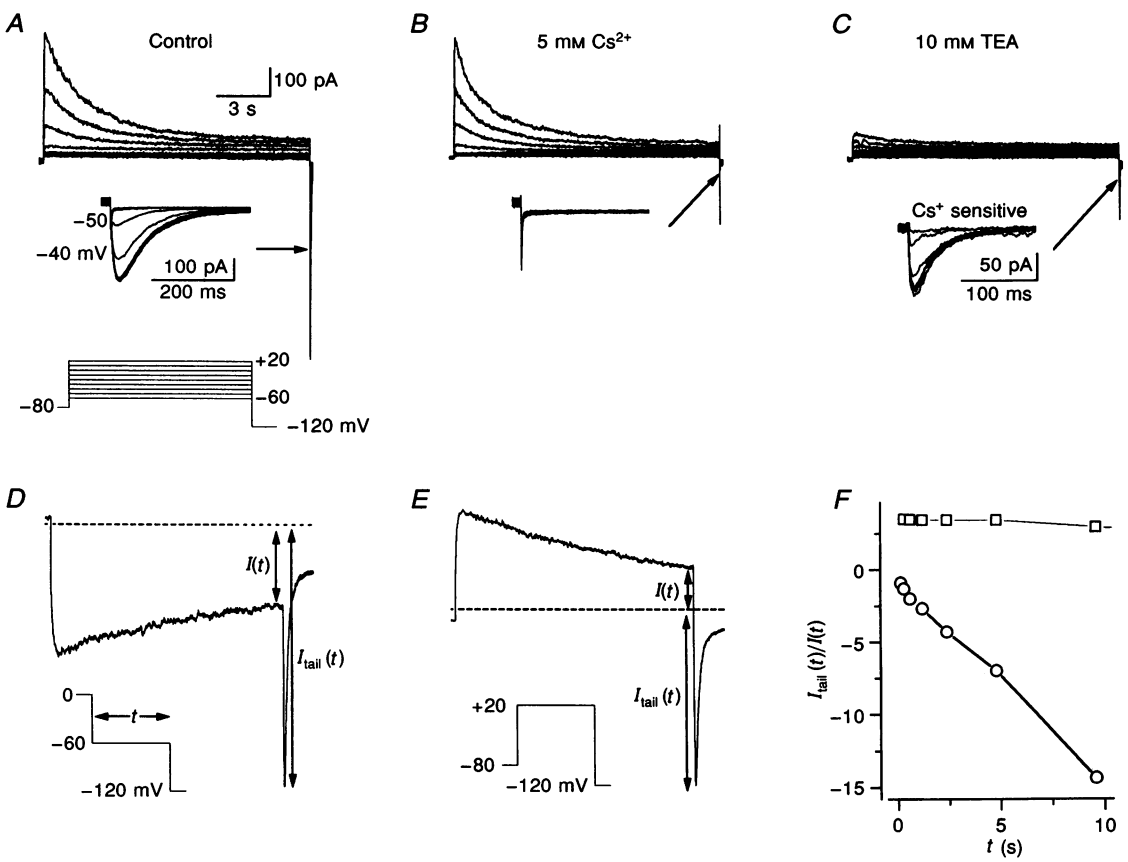

Figure 2. Outward currents in F-11 cells: pharmacological and biophysical characterization

A, currents obtained in the range −60 to +20 mV from a holding potential of −80 mV (protocol below). Inset: large inward currents elicited at −120 mV. *B*, same as *A* but after application of 5 mM Cs^+. Inset: note the disappearance of the inward currents elicited at −120 mV. Recovery was complete (not shown). *C*, same as *A*, but after the application of 10 mM TEA. Inset: the currents elicited at −120 mV after subtracting the traces obtained from recordings in the presence of both Cs^+ and TEA. The traces are similar to those shown in *A*, but smaller, due to the TEA blockage of I_{IR}. *D* and *E*, typical recordings during the envelope of tails test with the indication of the procedure to determine the ratio $I_{tail}(t)/I(t)$ shown in the insets. Note the difference in the protocols applied. *F*, plot of the envelope of tails tests (see text) derived from experiments similar to those shown in *D* (□) and *E* (○). $[K^+]_o = 40$ mM.

that the cells depolarize in the presence of selective blockers of I_{IR} (see Fig. 3).

The action of antiarrhythmic blockers on inward and outward components of I_{IR}

A stringent clue to identifying I_{IR} as a HERG-like current was further pursued by using the class III antiarrhythmic agents E4031 and WAY. Indeed, both these agents strongly inhibited I_{IR} in all the tested cells (Fig. 3*A* and *B*, $n = 10$), while they did not affect the outward delayed rectifier currents (Fig. 3*C* and *D*). We then compared the effects of these blockers on V_{rest}, showing that, on F-11 cells, WAY has similar depolarizing effects to Cs^+ or high K^+ (Fig. 3*E–G*, $n = 4$). Analogous, but less strong, depolarizing effects were obtained with E4031 (not shown), a result which suggests that either this drug, as reported for I_{HERG} (Trudeau *et al.* 1995), is less effective on outward as compared with inward components of I_{IR}, or the E4031 activity is voltage dependent. The voltage dependence of E4031 and WAY blockage was explored by preconditioning the cells alternately at −90 or 0 mV for long periods of time (25 s), before eliciting I_{IR} (see protocol in Fig. 3*J*). After a 5 min application, E4031 (Fig. 3*H*) caused a voltage-dependent block of the current, while the block by WAY (Fig. 3*I*) turned out to be voltage independent.

These data, while stressing the physiological role of I_{IR}, indicate that this current displays a sensitivity to pharmacological treatments quite similar to that of $I_{K(r)}$. In fact not only the inward but also the outward component was inhibited by antiarrhythmic blockers in the case of $I_{K(r)}$, while E4031 was either totally ineffective on I_{HERG}

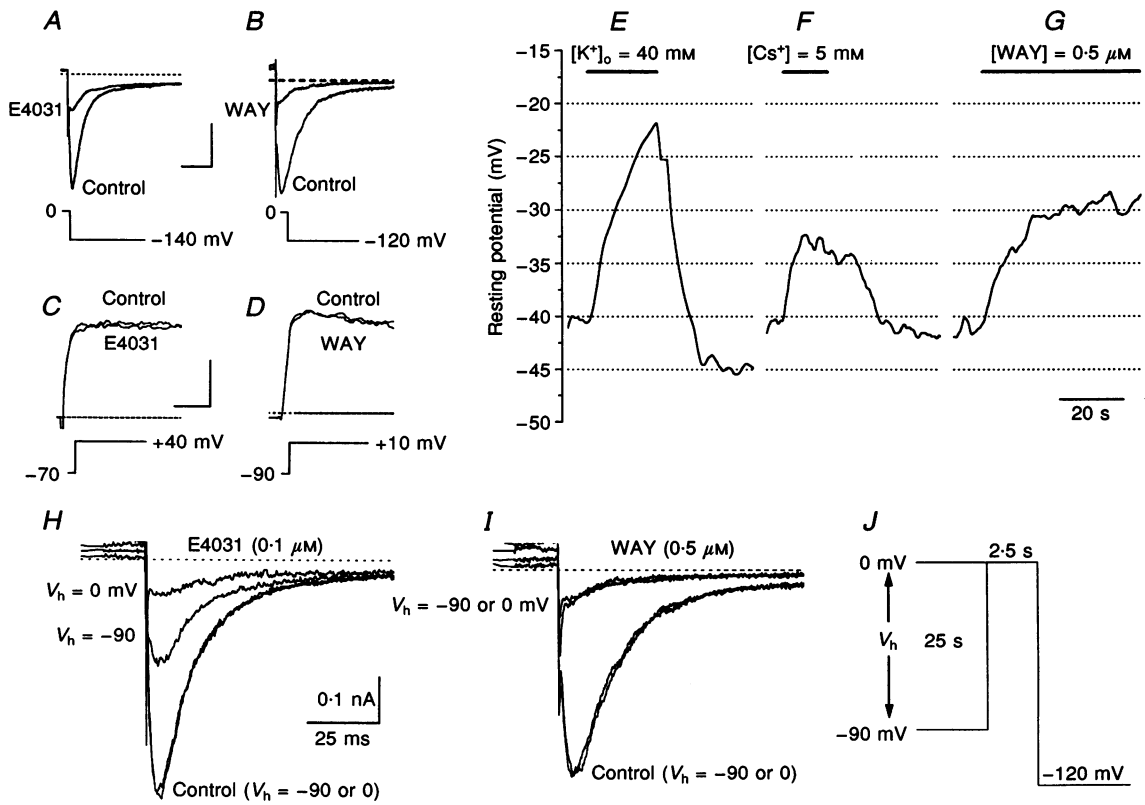

Figure 3. Pharmacological characterization of I_{IR}, with E4031 and WAY-123,398

A and *B*, traces from two different cells showing the inhibitory effect of 50 nM E4031 and 0·5 μM WAY, respectively, on I_{IR} (see protocols below). The two traces were obtained before (Control) and 180 s after drug addition. The residual decaying current during drug application is mainly due to imperfect compensation of the capacitive transient. Calibration: *A*, 400 pA, 25 ms; *B*, 200 pA, 25 ms. *C* and *D*, in the same two cells shown in *A–B*, the drug was ineffective on outward currents elicited according to the protocols shown below. Calibration: *C*, 200 pA, 100 ms; *D*, 50 pA, 100 ms. All data in *A–D* were obtained in 40 mM K^+_o. *E–G*, V_{rest} recorded in another cell in $[K^+]_o = 2$ mM during successive application (horizontal bars) of 40 mM K^+, 5 mM Cs^+ and 0·5 μM WAY. In *E* it is shown that a brief exposure to 40 mM K^+_o reversibly shifted V_{rest} from −40 to −22 mV. Addition of 5 mM Cs^+ (*F*) or WAY (*G*) produced similar depolarizing effects to those caused by elevating $[K^+]_o$. *H–J*, procedure to determine the voltage dependence of the drugs in two different cells. The protocol shown in *J* was applied in control and during a 5 min drug perfusion. In control, I_{IR} was independent from the long lasting V_h. For E4031 the blocking effect was smaller at $V_h = -90$ than at 0 mV (*H*). For WAY the blocking effect was voltage independent (*I*). $[K^+]_o = 40$ mM.

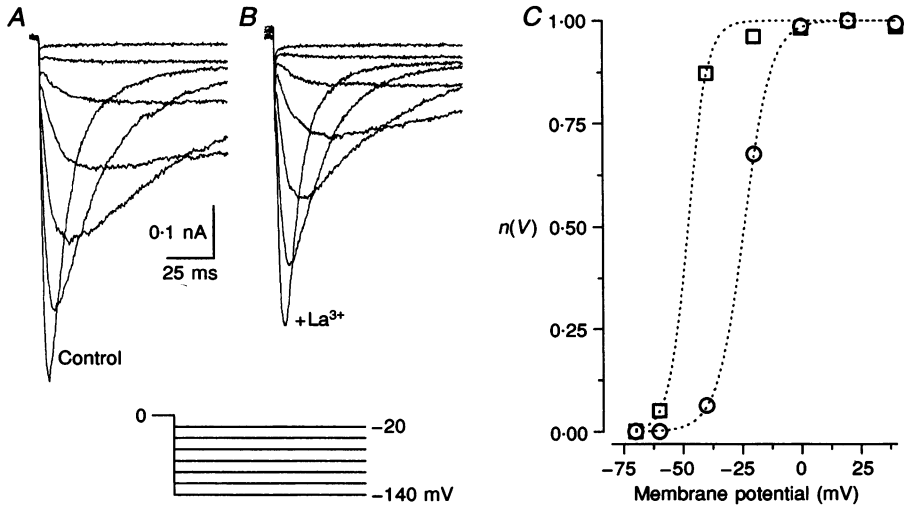

Figure 4. The effects of La^{3+} on I_{IR} from F-11 cells

A and *B*, I_{IR} recorded before (*A*) and after (*B*) application of 30 μM La^{3+}. Inhibition was completely reversible (not shown). *C*, plot of $n(V)$ in control and after the application of La^{3+} (□, control; ○, La^{3+}). Boltzmann curves (dotted lines) had the following parameters: $V_{½}$ from −47·9 to −24·3 mV, slope from 4·2 to 5·8 mV.

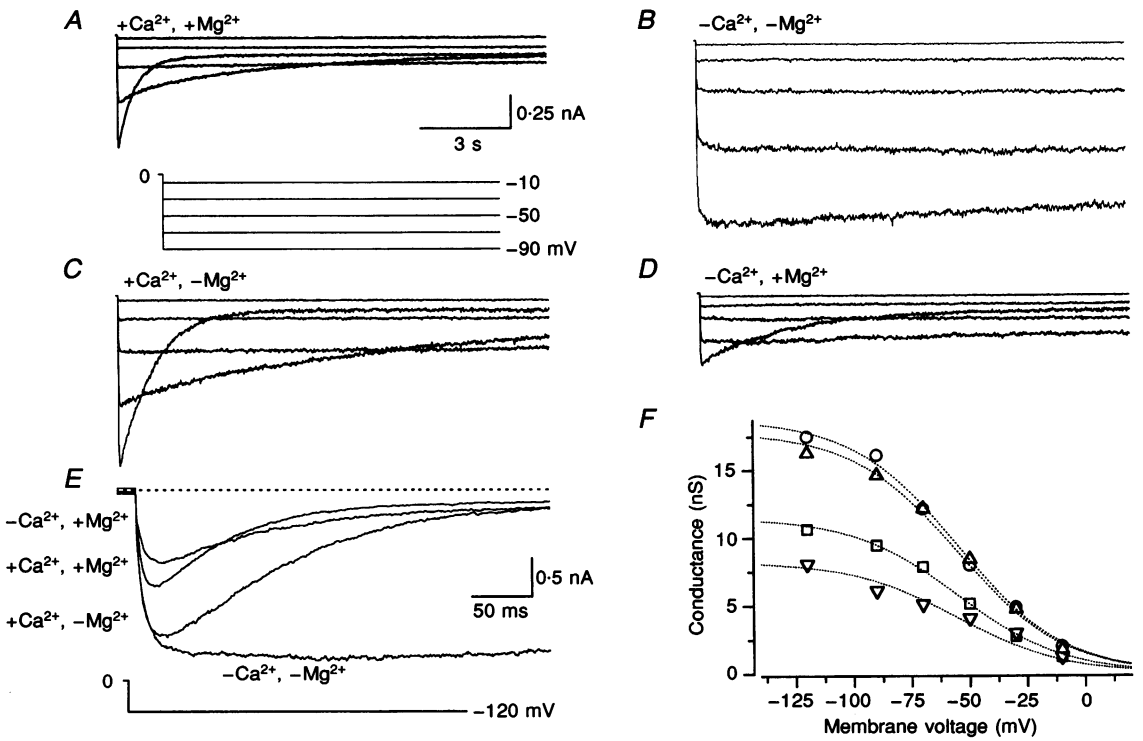

Figure 5. The effects of divalent cations in high K^+ solutions on the deactivation of I_{IR}

A, control recordings of I_{IR} elicited with the voltage protocol shown in the lower part of the panel in 120 mM K_o^+. *B*, same as in *A* but after 3 min perfusion with a solution of 120 mM K_o^+ and 5 mM EGTA. The I_{IR} deactivation is removed. *C*, the currents 2 min after re-addition of 2 mM Ca^{2+}. *D*, the currents 3 min after a wash with the 5 mM EGTA solution and subsequent re-addition of 2 mM Mg^{2+}. *E*, the superimposed recordings of the currents elicited at −120 mV from a holding potential of 0 mV in control and in the four manipulations shown in *A*–*D* (control: $+Ca^{2+}$, $+Mg^{2+}$; divalent free: $-Ca^{2+}$, $-Mg^{2+}$; 2 mM Ca^{2+}: $+Ca^{2+}$, $-Mg^{2+}$; 2 mM Mg^{2+}: $-Ca^{2+}$, $+Mg^{2+}$). Data were obtained from a single F-11 cell ($n = 5$). *F*, the maximal or peak chord conductances obtained from the data shown in *A*–*E* are plotted with different symbols (○, $-Ca^{2+}$, $-Mg^{2+}$; △, $+Ca^{2+}$, $-Mg^{2+}$; □, $+Ca^{2+}$, $+Mg^{2+}$; ▽, $-Ca^{2+}$, $+Mg^{2+}$). Dotted lines are the Boltzmann relationships which best fitted the data (see text).

(Sanguinetti *et al.* 1995, but see Spector, Curran, Keating & Sanguinetti, 1996), or only effective on its inward component (Trudeau *et al.* 1995).

The action of La^{3+} shifted $n(V)$ to the right

In order to further compare I_{IR} with $I_{K(r)}$ and I_{HERG} we tested La^{3+}, a cation known to block these currents (Sanguinetti & Jurkiewicz, 1990*b*; Sanguinetti *et al.* 1995). In F-11 cells La^{3+} produced a weak change in the peak currents elicited from 0 mV (Fig. 4*A* and *B*, $12 \pm 4\%$ decrease, $n = 4$). We also observed a decrease in the deactivation time constant which was accompanied by a pronounced right-shift of the $n(V)$ relationship (24 ± 4 mV, $n = 3$; 10 μM La^{3+} caused a shift of 12 mV (not shown)). This I_{IR} response to La^{3+} closely resembles the positive shift produced by this cation on the activation curves of $I_{K(r)}$ and I_{HERG} (Sanguinetti & Jurkiewicz, 1990*b*; Sanguinetti *et al.* 1995).

The modulation of the activation relationship $n(V)$ by extracellular divalent cations in high K_o^+ solutions

We know from previous studies (Arcangeli *et al.* 1995) that the removal of extracellular divalent cations produces a left-shift of $n(V)$, while I_{IR} deactivation is slowed in high external K_o^+. We further explored this observation by exposing F-11 cells to a divalent cation-free solution containing 120 mM K_o^+. As shown in Fig. 5*B* this treatment produced larger long-lasting currents devoid of deactivation. Interestingly, the separate re-addition of Ca^{2+} or Mg^{2+} affected the currents very differently (although in both cases reversibly). In fact Ca^{2+} simply restored the deactivation process (Fig. 5*C*), whereas Mg^{2+} also caused a strong blockage of channels (Fig. 5*D*). The chord conductance for the data shown in Fig. 5*A–D* was computed in Fig. 5*F*, which suggests that the experimental points can be well fitted to the same Boltzmann relationship ($V_{½} = -55$ mV, slope 23 mV) with properties similar to those described for $R(V)$. For the sake of clarity, the effects of these treatments are compared in Fig. 5*E*, which shows the superimposed traces elicited at −120 mV from a holding potential of 0 mV. This comparison indicates the following: the deinactivation kinetics seem influenced by divalent cations; the amplitude of the peak current is apparently unaffected by Ca^{2+} whereas it is strongly reduced by Mg^{2+}; and the deactivation kinetics are mainly controlled by Ca^{2+} in the absence of Mg^{2+}. Whatever the precise molecular mechanism of this manipulation, it is worthwhile stressing the similarity of the

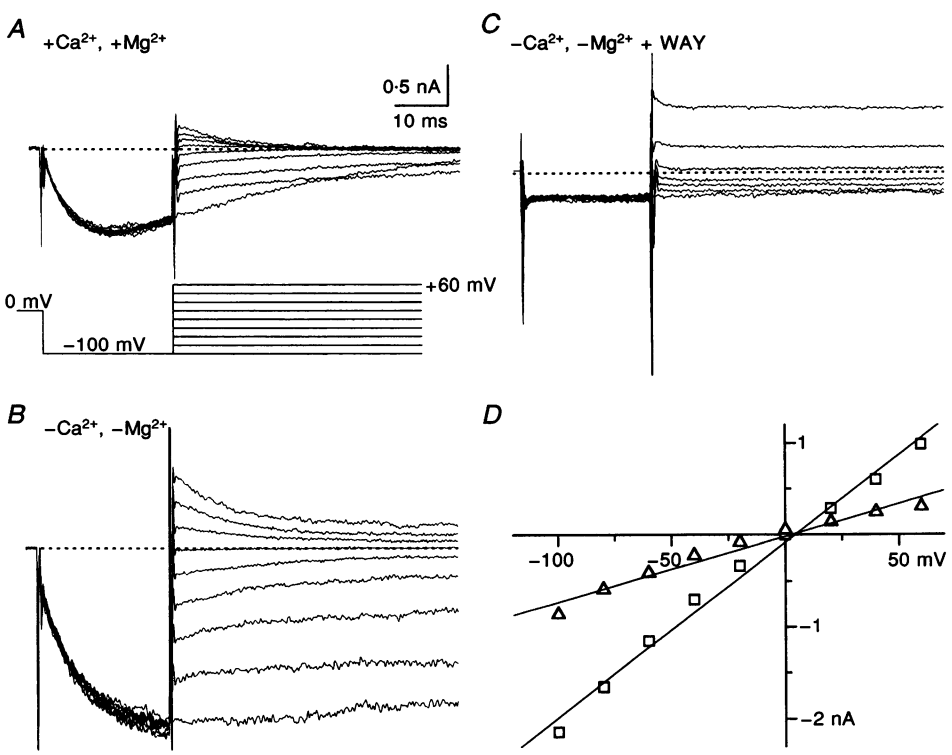

Figure 6. The open channel linear instantaneous current–voltage relationship in high K^+ solution with and without divalent cations

A, superimposed recordings of I_{IR} elicited according to the voltage protocol shown in the lower part of the panel. Traces are the result of the subtraction of data obtained in the presence of 1 μM WAY from data obtained without the drug. *B*, same as in *A* but in divalent-free solution (the recording of *C* was used). *C*, superimposed recording of currents obtained in the presence of WAY in divalent-free solutions. Notice the presence of outward delayed rectifier currents not blocked by the drug. *D*, the current–voltage relationships of the instantaneous currents shown in *A* (△) and *B* (□); the continuous lines across the points are the best fitting and correspond to conductances of 7 and 19 nS, respectively.

long-lasting currents of Fig. 5*B* with those of the triple-mutated ShB channel recently expressed in oocytes (Miller & Aldrich, 1996). In fact, the latter was interpreted as produced by the recovery from inactivation or, alternatively, in the tradition of the inward rectifier, as originating from a hyperpolarization activation.

I_{IR} has a non-rectifying permeation property

Since Smith *et al.* (1996) showed that the instantaneous current–voltage relationship of I_{HERG} is linear, we explored this property for I_{IR} either in control or divalent-free external solutions. The recordings shown in Fig. 6 represent the WAY-sensitive currents obtained after the subtraction of the currents recorded in the presence of 1 μM WAY (see the exemplary recordings in Fig. 6*C*) from the control recordings. The instantaneous I–V relationship shown in Fig. 6*D* is roughly linear, confirming that I_{IR} and I_{HERG} share this important feature. Moreover, the slope of the straight line corresponding to the divalent-free experiment indicates an increase in the conductance in keeping with the results shown in Fig. 5*F*. It is important to stress here that the long-lasting currents recorded in divalent-cation free solutions maintain the sensitivity to the antiarrhythmic drug WAY, suggesting that the cation subtraction does not affect this distinctive feature of the channel.

DISCUSSION

The major indication we draw from this work is that I_{IR} is a HERG-like current. If definitely proved, the expression of functional HERG channels in neuroblastoma cells would represent the demonstration that these types of structures are not only operative in the repolarization of heart muscle, but also have a physiological role in cells of neuronal lineage.

A unique kinetic model can describe I_{IR} as well as wild-type and mutant I_{HERG}

Sanguinetti's model defines currents as the product of an activation variable $n(V)$ and the inward rectification factor $R(V)$ (Fig. 7, uppermost left panel: $R(V)$, continuous line; $n(V)$, dotted line) according to eqn (1). The first column of Fig. 7 shows the qualitative features of the $n(V)$ and $R(V)$ relationships used to predict the outward (second column) and the inward (third column) currents of the following HERG-type channels: (1) the I_{HERG} expressed in oocytes or mammalian cells (first row); (2) the point-mutated channels produced by Schönherr & Heinemann (1996) or the double mutation of Smith *et al.* (1996) (S631A, second row); (3) the I_{IR} (third row, I_{IR}, this paper) and (4) the I_{IR} in the presence of solutions devoid of divalent cations (fourth row, see Fig. 5*B*). As shown, for all these channels, the $n(V)$ and $R(V)$ gates are Boltzmann curves, simply shifted along the voltage axis (see the rate constants in Methods), which differ in their $V_{½}$ values (see legend to Fig. 7). In Sanguinetti's model, the curves of the S631A row were simulated by only leaving the activation gate, $n(V)$, as illustrated. The predicted outward and inward currents correspond very well to those experimentally obtained by Sanguinetti *et al.* (1995). Moreover, by a simple shift of the voltage-dependent gates, Sanguinetti's model was perfectly suited to describe the extremely small outward and large inward I_{IR}. A less straightforward application of the model was necessary to predict I_{IR} in divalent-free solutions. To achieve this, it was in fact necessary to remove (or largely left-shift) the activation gate, leading to the intriguing possibility that, in the absence of divalent cations, the I_{IR} channel could be fixed in an open state, although maintaining the inactivation features. This lack of deactivation makes I_{IR} apparently very similar to the plant inward-rectifying channel KAT1 (Schachtman, Schroeder, Lucas, Anderson & Gaber, 1992). Since under these conditions the current is still blocked by antiarrhythmic drugs (see legend to Fig. 6) and Ca^{2+} and Mg^{2+} are effective in different ways, we suggest that divalent cations modulate rather specifically the activation gate by acting on the extracellular domains of the channel. This suggestion, however, is not easy to reconcile with the report that HERG deactivation kinetics are apparently regulated by an intracellular N-terminal domain (Schönherr & Heinemann, 1996). In conclusion, these qualitative comparisons between various expressed, mutated, natural and pharmacologically treated currents belonging to the HERG family fit perfectly the conclusions reached by Miller & Aldrich (1996, their Fig. 2) concerning the molecular transformation of outwardly rectifying into inwardly rectifying channels.

Similarities and dissimilarities between I_{IR} and $I_{K(r)}$

So far, $I_{K(r)}$ represents the only described HERG-like current constitutively operating in mammalian cells and thus represents the most appropriate available reference to which I_{IR} should be compared. Keeping in mind that the previous model adopted to describe I_{IR} was specular to that of Sanguinetti & Jurkiewicz (1990*a*), $m(V)$ and $h(V)$ of I_{IR} reported in Arcangeli *et al.* (1995) should be compared to $R(V)$ and $n(V)$ of $I_{K(r)}$, respectively. In Table 1 the Boltzmann parameters characterizing the voltage dependencies of I_{IR} from various neuroblastoma cell lines are compared with the corresponding parameters of $I_{K(r)}$ reported in the literature. On the whole, the two sets of values fall within very similar ranges, indicating that, whatever the interpreting model, the two types of currents are similar.

In agreement with this indication the pharmacological profile of I_{IR} practically coincides with that reported for $I_{K(r)}$, being sensitive to E4031, WAY and La^{3+} (Table 1). In fact I_{IR} is even more sensitive to E4031 than $I_{K(r)}$, so that a total block of the current is already obtained at 100 nM.

The only major difference between I_{IR} and HERG-type currents lies in the fact that the outward component of I_{IR} is negligible in comparison with the inward currents. We do not know if this discrepancy is due to tissue-specific or cell type-specific differences. However, the biophysical differences between $I_{K(r)}$ and I_{IR} are consistent with the roles played by these currents in the heart potential repolarization and in setting V_{rest} in neuroblastoma cells, respectively. No other

HERG-like current has been reported so far, apart from that described in pituitary tumour GH3 cells (Bauer, Meyerhof & Schwarz, 1990), which is very similar (blocked by E4031, our unpublished results) to I_{IR}, and a current characterized in a nematode muscle cell (Byerly & Masuda, 1979), endowed with properties of activation and inactivation resembling those described here.

From the theoretical point of view our complete model reveals that it is possible to obtain substantial outward current with an inward-rectifier channel simply by shifting to the right the Boltzmann relationships characterizing the voltage-dependent gates (Fig. 7). In other words, it is quite possible that I_{IR} differs from the $I_{K(r)}/I_{HERG}$ family essentially for a different area and position of the bell-shaped region corresponding to the so-called 'window current'.

Comparison between I_{IR} and I_{HERG}

Reported I_{HERG} currents have been obtained by expressing in oocytes or transfecting in mammalian cells the same *HERG* cDNA from human hippocampus, apparently encoding the major subunit forming $I_{K(r)}$ channels. Interestingly, these

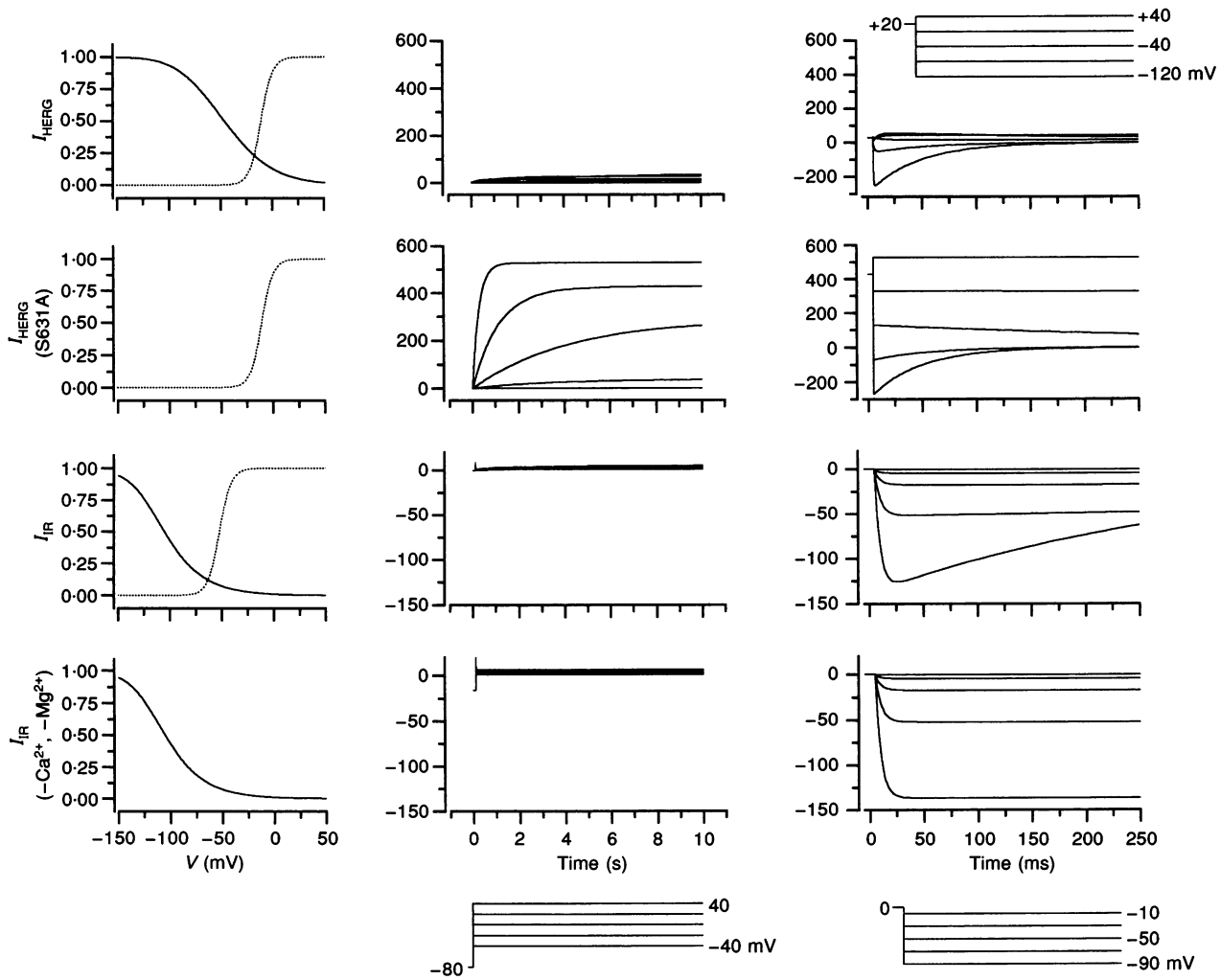

Figure 7. The comprehensive model that predicts I_{HERG}, mutated I_{HERG} (S631A), I_{IR} and I_{IR} in divalent-free solutions

Left-hand column, voltage-dependent gates $n(V)$ (dotted line) and $R(V)$ (continuous line) in the four indicated instances. The traces were derived from rates shown in Methods and approximately fitted to Boltzmann curves which differ in their $V_{½}$ values by 57 mV ($R(V)$) and 41 mV ($n(V)$) (see Table 1). Middle column, outward currents predicted according to the gates shown in the left-hand column and elicited with the voltage protocol shown in the lower part of the column. Right-hand column, inward currents predicted with the voltage protocols shown in the upper or lower part of the column. First row, data predicted for I_{HERG} expressed in oocytes or transfected cells (see text). Second row, data predicted for the S631A point mutation (see text). Only the $n(V)$ gate was used. Third row, data predicted for the I_{IR} described in the present paper. Fourth row, data predicted with the $R(V)$ gate and corresponding to experimental recordings shown in Fig. 5. $[K^+]_o$ was assumed to be 10 and 120 mM in the two upper and lower rows, respectively; $[K^+]_i$ was assumed to be 135 mM; vertical scales are arbitrary units but maximal conductances were assumed to be identical in the whole figure and not dependent on $[K^+]_o$.

Table 1. Comparison of gating and pharmacological properties of HERG-like channels and proposed descriptive models

Cell type or model	Property								
	$R(V)$ or $m(V)$		$n(V)$ or $h(V)$			Pharmacology			
	$V_{½}$ (mV)	Slope (mV)	$V_{½}$ (mV)	Slope (mV)	$g[K^+]_o$	IC_{50} of E4031 (nM)	IC_{50} of WAY (nM)	La^{3+}	Cs^+, Ba^{2+}
F-11[a]	−57·4	24	−52	4·8	SqRt	< 25	~200	+	+
SY5Y[b]	−49	18	−25	7·5	SqRt	< 30[c]	~250[c]	+	+
41A3[b]	−49	18	−42	4·7	SqRt	n.d.	n.d.	n.d.	+
N18TG2[c]	−52	19	−35	5·1	SqRt	n.d.	n.d.	n.d.	+
Submodel IR (3rd row, Fig. 7)[a]	−103	18	−52	5·6	—	—	—	—	—
Submodel HERG (1st row, Fig. 7)[a]	−46	23	−11	5·6	—	—	—	—	—
$I_{K(r)}$ (guinea pig)[d]	−9	22	−22	7·5	n.d.	400	n.d.	+	n.d.
$I_{K(r)}$ (rabbit)[e]	−68	n.d.	−25	7·4	SqRt	n.d.	n.d.	n.d.	n.d.
$I_{K(r)}$ (AT-1)[f]	n.d.	n.d.	+1	n.d.	n.d.	n.d.	n.d.	+	n.d.
$I_{K(r)}$ (cat)[g]	n.d.	n.d.	n.d.	n.d.	n.d.	n.d.	< 300	n.d.	n.d.
I_{HERG}[h]	−49	28	−15	7·9	Lin	Not found	n.d.	+	n.d.
I_{HERG}[i]	n.d.	n.d.	+6	11·7	n.d.	588	n.d.	n.d.	+
I_{HERG}[j]	−90	26	n.d.	n.d.	n.d.	n.d.	n.d.	n.d.	n.d.
I_{HERG}[k]	n.d.	n.d.	−19·5	n.d.	n.d.	n.d.	n.d.	n.d.	+

For submodels IR and HERG the half-point and slope data were derived after fitting curves in Fig. 7, left-hand column. [a]Present work, neuroblastoma; [b]Arcangeli *et al.* (1995), neuroblastoma; [c]L. Faravelli & E. Wanke, unpublished observations, neuroblastoma; [d]Sanguinetti & Jurkiewicz (1990*a*, *b*), guinea-pig; [e]Shibasaki (1987), rabbit; [f]Yang *et al.* (1994), mouse atrial tumour line; [g]Spinelli *et al.* (1993), cat; [h]Sanguinetti *et al.* (1995), oocytes; [i]Trudeau *et al.* (1995), oocytes; [j]Smith *et al.* (1996), HEK293 cell transient transfection; [k]Schönherr & Heinemann (1996), oocytes. The effects of inhibitors are compared on the basis of the relative concentration giving 50% inhibition of the current (IC_{50}). SqRt, square root; Lin, linear; n.d., not detected; +, active; $V_{½}$, mid-point of Boltzmann relationship; $g[K^+]_o$, $[K^+]_o$ dependence of conductance.

currents, although maintaining the biophysical features of $I_{K(r)}$, display substantial differences in their response to pharmacological agents (see Table 1). In fact, Sanguinetti *et al.* (1995) found their I_{HERG} current totally insensitive to E4031, while this inhibitor blocked only the inward component of the I_{HERG} described by Trudeau *et al.* (1995). These differences are probably due to different experimental conditions (voltage step protocols, composition of solutions, amount of cRNA injected). A more subtle difference between I_{IR} and I_{HERG} might be pointed out in the $[K^+]_o$ dependence of the chord conductance, which was found to be proportional to the square root of $[K^+]_o$ for I_{IR} (Arcangeli *et al.* 1995) and directly proportional to $[K^+]_o$ for I_{HERG} (Sanguinetti *et al.* 1995); it is, however, worth noting here that the square root law was verified for $I_{K(r)}$ (Shibasaki, 1987).

Conclusions

On the whole, differences within I_{HERG} and between these and $I_{K(r)}$ indicate that the *HERG* family is composed of currents sufficiently variable to include the peculiarities of I_{IR} described in this paper. This variability might depend, apart from experimental conditions, on differences in subunit co-assembly and/or tissue specific cofactors. It is important to note here that the inward rectification properties of KAT1 channels have been located in the region between the N-terminus and the end of the S4–S5 linker, where some specific charged residues absent in *Sh* families are present (Cao, Crawford & Schroeder, 1995). Since the amino acid identity between ion channel families shows that *HERG* is more closely related to *KAT1* (24%) than to the *Sh* family (12%; Warmke & Ganetzky, 1994), we cannot exclude the possibility that the properties of HERG channels derive directly from KAT1.

The identification of I_{IR} as a HERG-like current is now supported by the complete similarity of the so-far (90%) sequenced gene encoding for the I_{IR} in other neuroblastoma cells (SH-SY5Y) with the human hippocampal HERG (A. M. Brown, personal communication).

In this light our data provide new clues to enable the role of HERG channels in cells other than ventricular myocytes (particularly cells of the neuronal lineage) to be unravelled. In fact, in neuroblastoma cells the voltage dependence of I_{IR}

is somehow linked to the regulating machinery of the cell cycle (Arcangeli *et al.* 1995), and its activation is crucial for the signalling of neuritogenesis elicited by integrin-mediated adhesion on the protein components of the extracellular matrix (Arcangeli *et al.* 1993). Furthermore, we have evidence that I_{IR} is transiently expressed in normal nerve and muscle cells at very early stages of development and before differentiation (Wanke, Arcangeli, Olivotto, Bianchi & Faravelli, 1995; E. Wanke, A. Arcangeli, M. Olivotto, L. Bianchi, & L. Faravelli, unpublished observations).

ARCANGELI, A., BECCHETTI, A., MANNINI, A., MUGNAI, G., DE FILIPPI, P., TARONE, G., DEL BENE, M. R., BARLETTA, E., WANKE, E. & OLIVOTTO, M. (1993). Integrin-mediated neurite outgrowth in neuroblastoma cells depends on the activation of potassium channels. *Journal of Cell Biology* **122**, 1131–1143.

ARCANGELI, A., BIANCHI, L., BECCHETTI, A., FARAVELLI, L., CORONNELLO, M., MINI, E., OLIVOTTO, M. & WANKE, E. (1995). A novel inward-rectifying K^+ current with a cell-cycle dependence governs the resting potential of mammalian neuroblastoma cells. *Journal of Physiology* **489**, 455–471.

BAUER, C. K., MEYERHOF, W. & SCHWARZ, J. R. (1990). An inward-rectifying K^+ current in clonal rat pituitary cells and its modulation by thyrotrophin-releasing hormone. *Journal of Physiology* **429**, 169–189.

BOLAND, L. M. & DINGLEDINE, R. (1990). Multiple components of both transient and sustained barium currents in a rat dorsal root ganglion cell line. *Journal of Physiology* **420**, 223–245.

BYERLY, L. & MASUDA, M. O. (1979). Voltage-clamp analysis of the potassium current that produces a negative-going action potential in *Ascaris* muscle. *Journal of Physiology* **288**, 263–284.

CAO, Y., CRAWFORD, N. M. & SCHROEDER, J. I. (1995). Amino terminus and the first four membrane-spanning segments of the *Arabidopsis* K^+ channel KAT1 confers inward rectification property of plant–animal chimeric channels. *Journal of Biological Chemistry* **270**, 17697–17701.

CURRAN, M. E., SPLAWSKI, I., TIMOTHY, K. W., VINCENT, G. M., GREEN, E. D. & KEATING, M. K. (1995). A molecular basis for cardiac arrhythmia: HERG mutations cause long QT syndrome. *Cell* **80**, 795–804.

HODGKIN, A. L. & HUXLEY, A. F. (1952). Currents carried by sodium and potassium ions through the membrane of the giant axon of *Loligo*. *Journal of Physiology* **116**, 449–472.

MILLER, A. G. & ALDRICH, R. W. (1996). Conversion of a delayed rectifier K^+ channel to a voltage-gated inward rectifier K^+ channel by three amino acid substitutions. *Neuron* **16**, 853–858.

NOBLE, D. & TSIEN, R. W. (1969). Outward membrane currents activated in the plateau range of potentials in cardiac Purkinje fibres. *Journal of Physiology* **200**, 205–231.

PLATIKA, D., BOULOS, M. H., BAIZER, L. & FISHMAN, M. C. (1985). Neuronal traits of clonal cell lines derived by fusion of dorsal root ganglia neurons with neuroblastoma cells. *Proceedings of the National Academy of Sciences of the USA* **82**, 3499–3503.

SANGUINETTI, M. C., JIANG, C., CURRAN, M. E. & KEATING, M. T. (1995). A mechanistic link between an inherited and acquired cardiac arrhythmia: *HERG* encodes the I_{Kr} potassium channel. *Cell* **81**, 299–307.

SANGUINETTI, M. C. & JURKIEWICZ, N. K. (1990*a*). Two components of cardiac delayed rectifier K^+ current. *Journal of General Physiology* **96**, 195–215.

SANGUINETTI, M. C. & JURKIEWICZ, N. K. (1990*b*). Lanthanum blocks a specific component of I_K and screens membrane surface charge in cardiac cells. *American Journal of Physiology* **259**, H1881–1889.

SCHACHTMAN, D. P., SCHROEDER, J. I., LUCAS, W. J., ANDERSON, J. A. & GABER, R. F. (1992). Expression of an inward-rectifier potassium channel by the *Arabidopsis* KAT 1 cDNA. *Science* **28**, 1654–1657.

SCHÖNHERR, R. & HEINEMANN, S. H. (1996). Molecular determinants for activation and inactivation of HERG, a human inward rectifier potassium channel. *Journal of Physiology* **493**, 635–642.

SHIBASAKI, T. (1987). Conductance and kinetics of delayed rectifier potassium channels in nodal cells of the rabbit heart. *Journal of Physiology* **387**, 227–250.

SMITH, P. L., BAUKROWITZ, T. & YELLEN, G. (1996). The inward rectification mechanism of the HERG cardiac potassium channel. *Nature* **379**, 833–836.

SPECTOR, P. S., CURRAN, M. E., KEATING, M. T. & SANGUINETTI, M. C. (1996). Class III antiarrhythmic drugs block HERG, a human cardiac delayed rectifier K^+ channel. *Circulation Research* **78**, 499–503.

SPINELLI, W., MOUBARAK, I. F., PARSONS, R. W. & COLATSKY, T. J. (1993). Cellular electrophysiology of WAY 123,398, a new class III antiarrhythmic agent: specificity and frequency-independence of I_K block in cat ventricular myocytes. *Cardiovascular Pharmacology* **27**, 1580–1589.

TRUDEAU, M. C., WARMKE, J. W., GANETZKY, B. & ROBERTSON, G. A. (1995). HERG, a human inward rectifier in the voltage-gated potassium channel family. *Science* **269**, 92–95.

WANKE, E., ARCANGELI, A., OLIVOTTO, M., BIANCHI, L. & FARAVELLI, L. (1995). A novel K^+ inward rectifying current endowed with an intrinsic inactivation and a $(V - E_K)$-independent activation is present in neoplastic and immature cells from excitable tissues. *Society of Neuroscience Abstracts* **21**, 504.

WARMKE, J. W. & GANETZKY, B. (1994). A family of potassium channel genes related to *eag* in *Drosophila* and mammals. *Proceedings of the National Academy of Sciences of the USA* **91**, 3438–3442.

YANG, T., WATHEN, M. S., FELIPE, A., TAMKUN, M. M., SNYDERS, D. J. & RODEN, D. M. (1994). K^+ currents and K^+ channel mRNA in cultured atrial cardiac myocytes (AT-1 cells). *Circulation Research* **75**, 870–878.

Acknowledgements

The authors are indebted to Professors A. Ferroni and A. Fonnesu for their support, to Dr A. Zaza for suggesting the use of WAY-123,398 and E4031, to Drs A. Bacci, E. Pravettoni and N. Chiesa for help in some experiments, and to G. Mostacciuolo and M. Cutrì for crucial technical improvements. This work was supported by grants from the Associazione Italiana per la Ricerca sul Cancro (AIRC), Consiglio Nazionale delle Ricerche (CNR, Finalized Project ACRO), Ministero dell'Università e della Ricerca Scientifica e Tecnologica (MURST), Associazione Italiana contro le Leucemie (AIL). L.F. is a PhD student from Dipartimento di Fisiologia e Biochimica Generali, Università di Milano.

Author's email address

E. Wanke: wanke@imiucca.csi.unimi.it

Received 19 March 1996; accepted 14 June 1996.